small methods
www.small-methods.com

# Transient X-Ray Absorption Near Edge Structure Spectroscopy Using Broadband Free-Electron Laser Pulses

*Pavle Juranić,* Claudio Cirelli,* Talgat Mamyrbayev, Yohei Uemura, Joan Vila-Comamala, Frederico Alves Lima, Camila Bacellar, Philip J. M. Johnson, Eduard Prat, Sven Reiche, Anna Wach, Iuliia Bykova, Victoria Kabanova, Christopher Milne, and Christian David**

**A new method for time-resolved X-ray absorption near edge structure (XANES) spectroscopy that enables faster data acquisition and requires smaller sample quantities for high-quality data, thus allowing the analysis of more samples in a shorter time is introduced. The method uses large bandwidth free electron laser pulses to measure laser-excited XANES spectra in transmission mode. A beam-splitting grating configuration allows simultaneous measurements of the spectra of the incoming X-ray Free Electron Laser (XFEL) pulses and transmission XANES, which is crucial for compensating the pulse-dependent intensity and spectrum fluctuations due to the self-amplified spontaneous emission operation. The implementation of this new methodology is applied on a liquid solution of ammonium iron(III) oxalate jet and is compared to previous results, showing great improvements in the speed of acquisition and spectral resolution, and the ability to measure a large 2-D spectral-time map quickly.**

## 1. Introduction

X-ray absorption near edge structure (XANES) spectroscopy is a powerful technique that provides both electronic and structural information on the local environment around an absorbing atom.[1] By tuning the X-ray photon energy to be resonant with the element absorption edge of interest, it can probe the sample with chemical sensitivity, providing information from the perspective of the various species that compose the material. This method is applied to a range of different substances, including liquid, gas-phase, and solid-state samples. This flexibility has made XANES a popular technique for users of accelerator-based X-ray facilities and tabletop X-ray sources. One particular type of experiment that has taken full advantage of the information provided by this technique is time-resolved X-ray spectroscopy in which the sample is photo-excited with ultrafast laser pulses and subsequently probed using XANES. These techniques were first developed almost two decades ago[2–6] and have been implemented at a variety of light sources around the world.[7–12] The measurements have been used in a range of research fields, including chemistry, biology, and material science. With the introduction of intense femtosecond X-ray pulses at X-ray Free Electron Lasers (XFELs)[13–19] that can be synchronized with an external optical laser, XANES has moved into the femtosecond time domain,[20] allowing the ultrafast dynamics to be investigated in systems such as spin-crossover molecular species,[21–23] photo catalytically active materials,[24–27] and metalloporphyrin-based proteins.[28–30] This step from synchrotron to XFEL measurements enabled researchers to execute pump-probe XANES measurements, creating an active field of research in recent years.

The biggest challenge to the implementation of the XANES technique at XFELs[20] has been the requirement to scan the photon energy of the incident beam to obtain a complete X-ray absorption spectrum. While XANES measurements at synchrotrons are routine due to the high long-term stability of the X-ray beam, the XFEL pulses are characterized by strong shot-to-shot fluctuations in both their intensity and energy spectrum due to the self-amplified spontaneous emission (SASE) process that generates the XFEL radiation in most XFELs around the world. These fluctuations significantly hinder the normalization of the XANES spectrum versus the incoming spectrum across any kind of data acquisition that utilizes a monochromator or energy scan at XFELs. The combination of an easily normalized spectrum and a short intense X-ray pulse useful for pump-probe XANES has so far been difficult to achieve at synchrotrons and at XFELs.

P. Juranić, C. Cirelli, J. Vila-Comamala, C. Bacellar, P. J. M. Johnson, E. Prat, S. Reiche, A. Wach, I. Bykova, V. Kabanova, C. David
Paul Scherrer Institute
Forschungsstrasse 111, Villigen 5232, Switzerland
E-mail: pavle.juranic@psi.ch; claudio.cirelli@psi.ch; christian.david@psi.ch

T. Mamyrbayev
XRnanotech GmbH, PSI
Forschungsstrasse 111, Villigen 5232, Switzerland

Y. Uemura, F. A. Lima, C. Milne
European XFEL GmbH
Holzkoppel 4, 22869 Schenefeld, Germany

The ORCID identification number(s) for the author(s) of this article can be found under https://doi.org/10.1002/smtd.202301328



**DOI: 10.1002/smtd.202301328**

Previous efforts to achieve these two goals were attempted at the SACLA XFEL (Japan) and at LCLS (California, USA). An attempt to overcome the spectral normalization issue was made at the SACLA XFEL, in which a diffraction grating followed by an X-ray mirror was used to create two copies of the SASE XFEL beam, allowing the sample to be measured using transmission XANES in one beam while the other is used as a reference for the X-ray spectrum.[31] This approach was applied in the study of femtosecond ligand disassociation dynamics in ammonium iron(III) oxalate in aqueous solution. However, the SACLA attempt was limited by the narrow bandwidth ΔE/E of 0.3% at 7.1 keV the SACLA XFEL provided, still requiring an energy scan to get a full XANES spectrum. In addition, the nonuniformity of the 2D X-ray detector used to measure the two dispersed X-ray spectra required further correction beyond simple normalization between the sample and reference measurement. Moreover, the 1 and −1 order diffraction efficiency of the gratings was only a few percent, making the method rather photon-inefficient. Another attempt to overcome the pump-probe XANES issues at XFELs was made at the LCLS XFEL using a dispersive X-ray spectrometer based on bent Si crystals[32] placed before and after the sample, allowing the incident and transmitted X-ray spectrum to be measured on a shot-by-shot basis while probing matter under extreme pressure.[33] However, this attempt also used a narrow bandwidth of the XFEL, with an ΔE/E of ≈1% at 2.5 keV, and was not used to measure ultrafast dynamics. Another measurement at LCLS with a relatively large bandwidth mode of ≈100 eV centered at the iron K edge was recently published.[34] This work employed a similar geometry as[32] and presents fluence-dependent statistic XANES data on iron foils. Further evaluations were done at SACLA, comparing the time-resolved XANES signal strengths measured in transmission and fluorescence.[35] This study concluded that fluorescent detection resulted in an efficiency of about an order of magnitude larger than the transmission mode method presented in[31] for monochromator scans. The method presented in this manuscript demonstrates that combining a higher grating transmission efficiency in the 1st and −1st order with a large incoming spectrum bandwidth leads to transmission mode being the most efficient choice for the time-resolved XANES measurements.

An ideal setup to maximize the efficiency of XANES measurements at an XFEL would combine the elements from the experiments at SACLA and LCLS with a large incoming spectrum bandwidth to get complete XANES spectra without the requirement for photon energy scanning. Recent developments by the SwissFEL beam dynamics group at the Paul Scherrer Institut (Switzerland) showed that this XFEL was capable of producing bandwidths of ≈3% ΔE/E.[36,37] In addition, the nanofabrication lab at the Paul Scherrer Institut, where SwissFEL is located, also developed more advanced methods for the manufacture of diamond gratings having improved transmission in the 1st and −1st order. These developments prompted the authors to attempt the optimized transmission XANES measurement experiment, with results that demonstrated that this methodology is more efficient and faster than previous XANES experiments at XFELs. The combination of more reliable detectors, a more efficient grating, a larger XFEL bandwidth, a spectrometer with a larger bandwidth acceptance, and better temporal resolution pushes this methodology from being a proof-of-principle concept to a viable experimental method that saves both time and sample quantity, thus enabling higher throughput user experiments.

## 2. Setup and Measurement

The experiment was carried out at the iron K-edge X-ray energy (7.112 keV) at the Alvra end station of SwissFEL, using their main experimental (Prime) chamber and the secondary (Flex) table setups.[38] The sample used was ammonium iron (III) oxalate, $(NH)_3Fe(C_2O_4)_3 \cdot 3\ H_2O$, in an aqueous solution comparable to the one used in the SACLA experiment.[39] To compare this experiment with previous results, we used a similar molar density for the sample of 500 mM in the liquid jet. The experimental setup is shown in **Figure 1**. The beam was focused by a pair of Kirkpatrick–Baez mirrors so that the slightly defocused beam at the sample jet plane had an illumination of 20 μm × 20 μm. The PRIME chamber was filled with helium at a pressure of 800 mbar. Prior to reaching the sample plane, the beam was split by a 600 nm period diamond transmission grating with 2.65 μm high structures. The first-order beam passed through the 100 μm thick liquid jet, while the negative first-order beam passed through the chamber without impinging on the sample. This second beam was used as the reference spectrum for normalization. During the XANES measurements, the grating was tilted[40] to 64° from the vertical to reach the optimum effective line height of 6 μm. In this condition, this setup delivered ≈40% of the beam in the 1st and −1st order beams each, and only ≈1% in the 0 order. The diamond grating was manufactured using high-resolution electron beam lithography and a deep reactive ion etching process, similar to the one described in ref. [41].

The two first-order beams exited the PRIME chamber through a diamond window to go to an in-air bent crystal spectrometer setup on the FLEX table. The spectrometer was made from a Si <110> bent crystal used in the <220> geometry with a radius of curvature of 12.8 mm mounted on a multi-directional mover stage that can also rotate the crystal. The spectra were observed by a detector setup consisting of a Ce:LuAG scintillating screen and a lens that images the screen onto a PCO.edge 5.5 camera. The detector system was located 100 mm from the surface of the bent crystal. The SwissFEL SASE pulses used in the experiment had a 3% ΔE/E bandwidth centered at 7.17 keV, with a pulse energy ≈740 μJ.[36] The FEL setup for the measurements did not have a spatial chirp, unlike that in.[36]

The pump laser used in the experiment is the Aramis endstation experimental laser at SwissFEL[38] was tuned to a central wavelength of 400 nm. It was focused down to a spot size of ≈44 μm by 37 μm, delivering ≈20.5 μJ of laser pulse energy, yielding a fluence of ≈1260 mJ $cm^{-2}$. The laser/X-ray pump-probe delay was set by a motorized stage on the laser arm of the experiment. An alignment screen and camera were set up downstream of the experiment for alignment.

The spectrum was optimized to produce a large bandwidth that covered the range between ≈7035 and 7260 eV, giving a bandwidth of 225 eV. A typical single-shot spectrum of the large bandwidth mode taken by the experiment spectrometer setup is shown in **Figure 2**. The spectrometer was calibrated by using a monochromator scan to retrieve a pixel-to-energy map along the dispersive direction of the camera sensor. The spectra were evaluated by summing up the signal on the spectrometer camera along

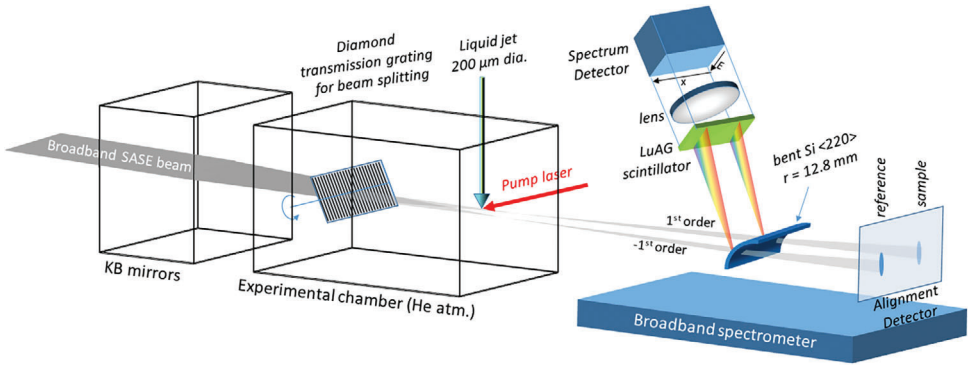


**Figure 1.** Experimental setup at the Alvra end-station at SwissFEL. The photon beam is passed through a transmission grating with one of the 1st order beams delivered to the sample liquid jet. The −1st order beam which does not travel through the liquid jet, is used for spectral measurements of the XFEL beam for shot-to-shot normalization. The spectra are dispersed by the bent Si <220> crystals onto a camera.

a region of interest of the nondispersive axis for each dispersive pixel position of the detector to produce a 1D spectrum, like the one shown in Figure 2. Two such regions of interest were set up on the camera detector, one for the signal spectrum, and one for the reference spectrum.

The experiment was conducted by running SwissFEL at 100 Hz repetition rate, and the laser at 50 Hz repetition rate. This allowed a comparison of the pumped and unpumped spectra on a pulse-to-pulse basis and also to normalize the 1st order transmission XANES spectra versus the −1st order measurement of the beam. We recorded 5000 of both pumped and unpumped spectra at each temporal delay step, with ≈10 delay steps per temporal scan. The differential XANES spectrum between excited and ground states is calculated on a shot-to-shot basis. These differential spectra are distributed along the time delay axis based on the arrival time of the timing tool and then averaged within a selectable delay step size (25 fs in **Figure 3**).[42] The average acquisition times were ≈10 min per XANES spectrum. Similar measurements done with a monochromator at the Alvra beamline at SwissFEL usually take several hours over the same energy range. The data was processed on a single-shot basis by first normalizing the pumped and unpumped XANES spectra between the reference and signal XFEL spectra on the spectrometer according to the equation.

$$S_{\mathrm{xas}} = -\ln\left(S_{\mathrm{ref}}/S_{\mathrm{sig}}\right) \tag{1}$$

where $S_{\mathrm{xas}}$ is the normalized XANES spectrum and the $S_{\mathrm{ref}}$ and $S_{\mathrm{sig}}$ are the reference spectrum and signal through the sample jet for each shot, respectively. We take the difference between the pumped and unpumped XANES spectra to observe the effect of the laser excitation for each time delay step sorted with the timing tool, and the spectra within that step are averaged. The equation used to find this effect per shot is

$$S_{\mathrm{diff}} = S_{\mathrm{xas\_pump}} - S_{\mathrm{xas\_upump}} \tag{2}$$

where $S_{\mathrm{diff}}$ is the difference between the $S_{\mathrm{xas\_pump}}$ and $S_{\mathrm{xas\_upump}}$ spectra, the pumped and unpumped XANES spectra, respectively. The resulting 2D XANES pump-probe map is shown in Figure 3. The 2D XANES pump-probe map recreates a 1D energy XANES transient spectrum at any time step when taken along a

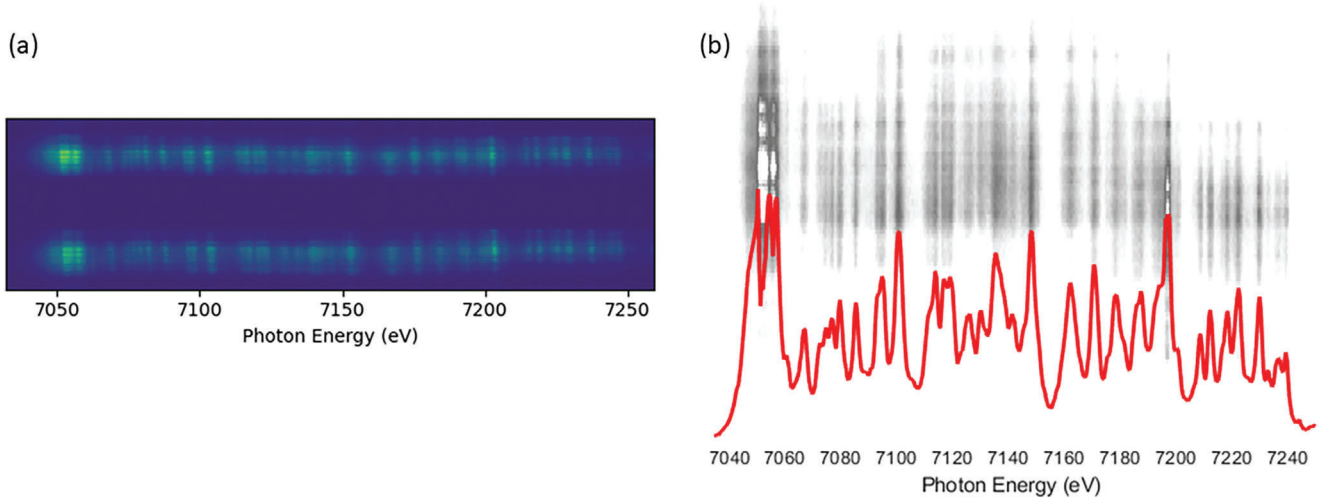


**Figure 2.** A typical single-shot large bandwidth spectrum camera shows the visible 1st and −1st order a), with the 0 order being almost completely suppressed. The 1st order spectrum and its 1D projection (red line) b).

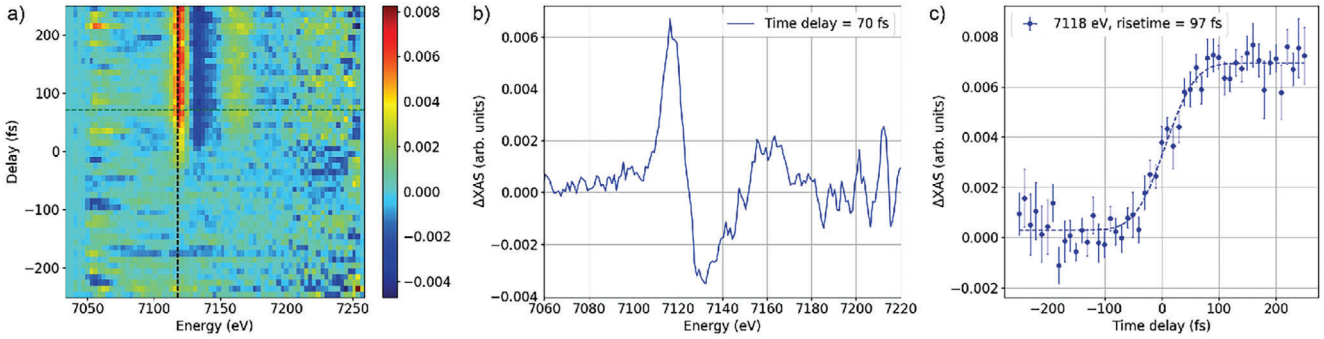


**Figure 3.** XANES pump-probe map of ammonium iron (III) oxalate. The 2D time-delay versus energy map with line projections along 7118 eV (red line, vertical) and 70 fs (blue line, horizontal) a). A XANES transient spectrum at 70 fs time delay b), and a kinetic trace extracted at the photon energy of 7118 eV with a fitting curve to determine the rise time c).

time step, and a pump-probe 1D graph when taken along a constant photon energy point with an energy acceptance window of 1 eV.

Before measuring on the liquid jet, the setup was characterized by measuring the K-edge XANES with an iron (Fe) foil of 6 µm thickness at 7112 eV. This static measurement was convenient to fully characterize the setup and determine the efficiency of the method proposed here. The measurement was compared to a reference spectrum from the X-ray Absorption Data Library (IXANES)[43] and the data taken by Matt Newville on the APS 20-BM-B beamline. Previous static measurements with foils at the Alvra end-station at SwissFEL have shown that the energy resolution of the scan is typically lower than the reference synchrotron data, and that is also visible in the measurement presented in **Figure 4**. The fluence we had at the experiment was $\approx 2*10^{15}$ W cm$^{-2}$, which was below the fluence threshold for the saturable absorption effects described and discussed in.[34,44] A slightly lower energy resolution at nonseeded X-ray FELs is expected due to the nature of the accelerator where position, energy, and intensity single-shot jitters, as well as long-term drifts of the X-ray beam properties can occur. The Fe K-edge XANES measurement shown here nicely matches the reference data in terms of position and the shape of the postedge features, but agrees less well for narrower features like the pre-edge shoulder and the white line peak. However, the resolution is sufficient to see time-dependent phenomena and demonstrate the method highlighted in this paper.

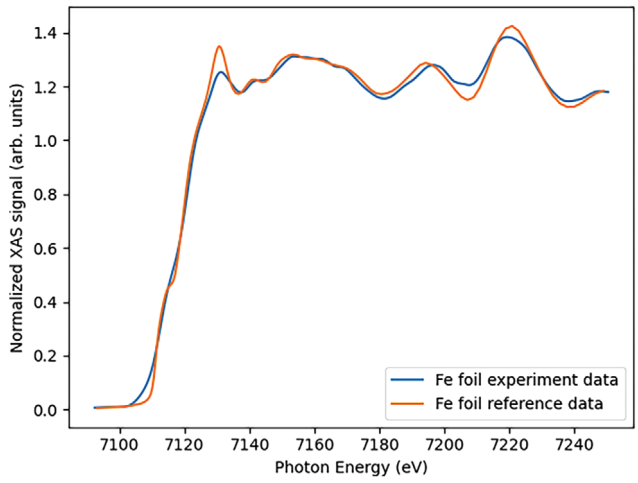


**Figure 4.** Comparison of the XANES Fe foil data from this experiment and that taken from a reference library from a synchrotron.

## 3. Result

The Fe K-edge XANES measurements presented here indicate that the method follows Poisson statistics, enabling an estimate of the method's effectiveness. The evaluation method consists of taking N shots at random from a very large dataset, calculating their averaged spectrum, and then inspecting the deviation of this averaged spectrum with respect to the spectrum calculated averaging the whole dataset. This is then repeated 100 times, selecting the N different spectra randomly every time. The evaluation, graphically shown in **Figure 5**, follows the expected $1/\sqrt{N}$, giving, for example, a deviation from the mean of ≈1% for 10 000 spectra.

The foil evaluations show that the quality of the data matches reference spectra. However, the discussion in[35] concluded that the fluorescence method is about an order of magnitude more efficient in producing signal relative to the number of input photons when compared to the transmission time-resolved XANES with an ΔE/E bandwidth of 0.3%. This evaluation has several caveats: the measurements were done with a smaller bandwidth than the method presented in this paper, and the 1st and −1st diffraction orders of the grating were an order of magnitude smaller than the 0 order. Both of these issues have been addressed in our setup, with the larger bandwidth of the SwissFEL pulses being at 3%, and the grating diffraction efficiency of the 1st and −1st order now being an order of magnitude higher than in earlier experiments, yielding an increase in X-ray flux per pulse of ≈400 times with respect to that in.[35] The transmission efficiency improvement changes the relative efficiency of the two methods, and the addition of the large bandwidth pushes the transmission time-resolved XANES further ahead.

The monochromator bandwidth that is required for these fluorescence measurements at Alvra is ≈0.02% (1.4 eV), meaning that ≈15 monochromator steps were needed to match the 0.3% (21.3 eV) bandwidth of the SASE pulses. Because the setup presented here has a 3% (200 eV) bandwidth, the same monochromator scans would need to be done 150 times to scan over the

 

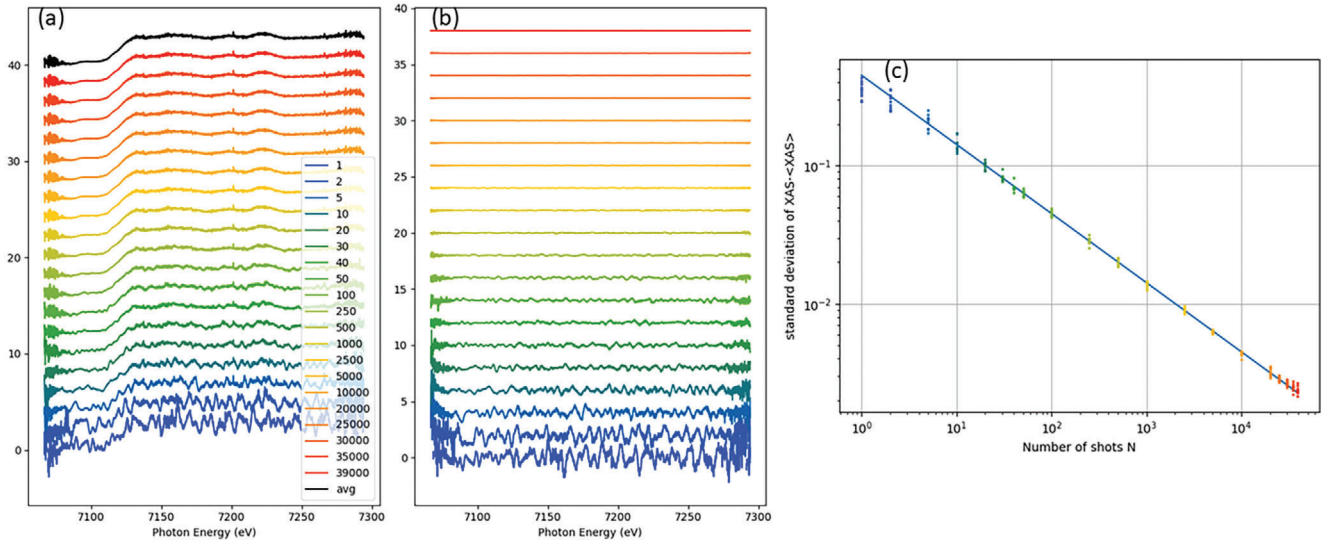


**Figure 5.** Evaluation of Fe foil measurements at 7112 eV. The average of the scan for a number of shots (1 shot to 39 000 shots) a), the difference between the averages of the subset and the whole data set b), and the relationship between the accuracy of the measurement versus the size of the selected subset of data c).

same energy range. In both cases, the method presented here is at least an order of magnitude faster than the monochromator measurement. Being able to do just a one-time scan for a large bandwidth also greatly mitigates issues with timing drifts that can occur in pump-probe experiments when forced to do the same time scan multiple times over several different photon energies. There is also less need for tuning the XFEL for different energies or scans, each step of which costs time during which the sample is either not being measured or wasted. For time-sensitive samples, the efficiency of being able to have a large bandwidth that does not need to be tweaked during the measurement, combined with having to do just a one-time scan to get the pump-probe data needed, enables a much faster experiment-to-data pipeline.

The resulting 2D time-energy XANES spectra can be used to evaluate the dynamics of the sample at any photon energy within the XFEL spectral bandwidth or observe the XANES transient at any measured time delay. The measurement reduced what was in the past done in two separate scans, one over time and one over photon energy,[39] to just one, and allowed for a higher spectral resolution of ≈1 eV. The spectrometer set up in this experiment allowed for the binning of the data along the energy axis in finer steps than the bandwidth of the beamline monochromator due to the camera pixel size, scintillator resolution, and spectrometer design. The efficiency of the methodology is very high and allows the experiment to take multiple runs of pump-probe data. The pump-probe kinetic trace in **Figure 6** took ≈15 min to measure and yielded XANES pump-probe data for several different photon

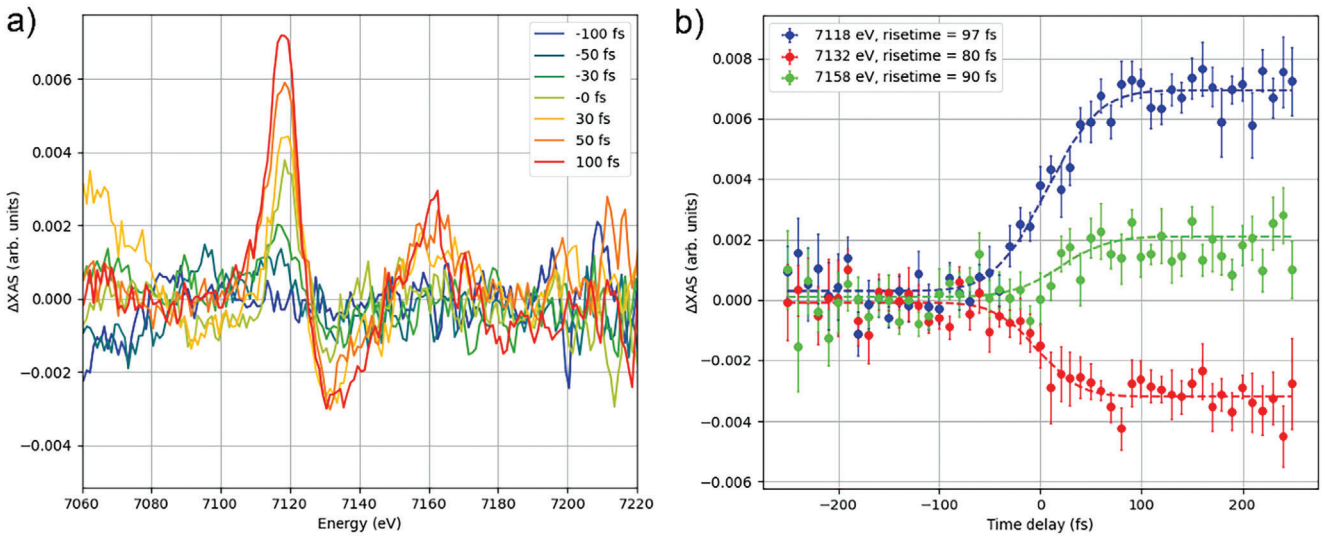


**Figure 6.** Pump-probe XANES spectra taken for iron (III) oxalate. A kinetic trace at several different time delays a), and a temporal scan from −250 to 300 fs sorted into 10 fs bins b) extracted from Figure 3.

energies. The experimental data show a rise time of ≈90 fs, being limited only by the experimental instrument response function (IRF) mainly induced by the XFEL and laser pulse durations. The experiment presented in[39] resulted in data roughly equivalent to our measurements shown in Figure 6, but it required several photon energy steps to cover ≈200 eV, each requiring a temporal scan, whereas the setup presented here required just one temporal scan. Our measurements also profit from better transmission efficiency, leading to shorter acquisition time points per time step to produce data with better statistics.

In addition to the increased efficiency of the setup, the fact that the data from these measurements provide a 2D signal-time-energy map allows researchers to more quickly identify edge features, interesting temporal phenomena, and energy shifts with any desired energy resolution. Once those effects are identified, a more focused scan over just the relevant parameter spaces is possible.

## 4. Conclusion

The transmission time-resolved XANES method presented in this paper enables faster, more efficient, and more detailed measurements of pump-probe samples at free electron lasers. The method's main advantage is the ability to acquire a full 2-D spectrum at once, taking more data points for the same resources as the standard fluorescence time-resolved XANES methods. When compared to fluorescence monochromator scan measurements, the method can cover an energy range at least an order of magnitude faster. While the full implementation of the method requires a high-quality grating and an XFEL with a stable and well-tuned large bandwidth mode, the experience at SwissFEL is that both of these conditions are well within the reach of technical and operational capability. Though the method is currently capable of performing well at tender and hard X-rays, it may be possible to apply it to softer X-rays under special circumstances, with high-efficiency gratings that can provide high-intensity 1st and −1st order beams. The biggest challenge in such cases is the transmission of the beam through a sample and the grating, but if these can be mitigated by choice of materials, sample thickness, or sample type, the method could be applicable beyond the X-ray range presented here. As more XFELs begin to offer these modes, such experiments could be performed more routinely. The gratings can be manufactured by any well-established lithography laboratory, and their implementation in the experiments could foster greater collaboration between nanomanufacturing and biology or chemistry research groups.

## Acknowledgements

The authors acknowledge the Paul Scherrer Institute, Villigen, Switzerland for the provision of free-electron laser beamtime at the Alvra instrument of the SwissFEL ARAMIS branch.

Open access funding provided by ETH-Bereich Forschungsanstalten.

## Conflict of Interest

The authors declare no conflict of interest.

## Data Availability Statement

The data that support the findings of this study are available on request from the corresponding author. The data are not publicly available due to privacy or ethical restrictions.

## Keywords

FEL, large bandwidth, spectroscopy, XANES

Received: September 29, 2023
Revised: February 2, 2024
Published online:

[1] C. L. Jeroen A. Van Bokhoven, *X-Ray Absorption and X-Ray Emission Spectroscopy: Theory and Applications*, John Wiley & Sons Ltd., Hoboken, NJ **2016**.
[2] C. Bressler, M. Chergui, *Chem. Rev.* **2004**, *104*, 1781.
[3] C. Bressler, M. Saes, M. Chergui, D. Grolimund, R. Abela, P. Pattison, *J. Chem. Phys.* **2002**, *116*, 2955.
[4] L. X. Chen, W. J. H. Jager, G. Jennings, D. J. Gosztola, A. Munkholm, J. P. Hessler, *Science.* **2001**, *292*, 262.
[5] M. Saes, C. Bressler, R. Abela, D. Grolimund, S. L. Johnson, P. A. Heimann, M. Chergui, *Phys. Rev. Lett.* **2003**, *90*, 047403.
[6] I. V. Tomov, D. A. Oulianov, P. L. Chen, P. M. Rentzepis, *J. Phys. Chem. B.* **1999**, *103*, 7081.
[7] B. Adams, M. Borland, L. X. Chen, P. Chupas, N. Dashdorj, G. Doumy, E. Dufresne, S. Durbin, H. Dürr, P. Evans, T. Graber, R. Henning, E. P. Kanter, D. Keavney, C. Kurtz, Y. Li, A. M. March, K. Moffat, A. Nassiri, S. H. Southworth, V. Srajer, D. M. Tiede, D. Walko, J. Wang, H. Wen, L. Young, X. Zhang, A. Zholents, *Synchrotron Radiat. News.* **2012**, *25*, 6.
[8] L. X. Chen, X. Y. Zhang, J. V. Lockard, A. B. Stickrath, K. Attenkofer, G. Jennings, D. J. Liu, *Acta Crystallogr. A.* **2010**, *66*, 240.
[9] F. A. Lima, C. J. Milne, D. C. V. Amarasinghe, M. H. Rittmann-Frank, R. M. V. D Veen, M. Reinhard, V.-T. Pham, S. Karlsson, S. L. Johnson, D. Grolimund, C. Borca, T. Huthwelker, M. Janousch, F. van Mourik, R. Abela, M. Chergui, *Rev. Sci. Instrum.* **2011**, *82*, 063111.
[10] A. M. March, A. Stickrath, G. Doumy, E. P. Kanter, B. Krässig, S. H. Southworth, K. Attenkofer, C. A. Kurtz, L. X. Chen, L. Young, *Rev. Sci. Instrum.* **2011**, *82*, 073110.
[11] D. Göries, B. Dicke, P. Roedig, N. Stübe, J. Meyer, A. Galler, W. Gawelda, A. Britz, P. Geßler, H. Sotoudi Namin, A. Beckmann, M. Schlie, M. Warmer, M. Naumova, C. Bressler, M. Rübhausen, E. Weckert, A. Meents, *Rev. Sci. Instrum.* **2016**, *87*, 053116.
[12] A. Britz, T. A. Assefa, A. Galler, W. Gawelda, M. Diez, P. Zalden, D. Khakhulin, B. Fernandes, P. Gessler, H. Sotoudi Namin, A. Beckmann, M. Harder, H. Yavas, C. Bressler, *J. Synchrotron Radiat.* **2016**, *23*, 1409.
[13] W. Ackermann, G. Asova, V. Ayvazyan, A. Azima, N. Baboi, J. Bähr, V. Balandin, B. Beutner, A. Brandt, A. Bolzmann, R. Brinkmann, O. I. Brovko, M. Castellano, P. Castro, L. Catani, E. Chiadroni, S. Choroba, A. Cianchi, J. T. Costello, D. Cubaynes, J. Dardis, W. Decking, H. Delsim-Hashemi, A. Delserieys, G. Di Pirro, M. Dohlus, S. Düsterer, A. Eckhardt, H. T. Edwards, B. Faatz, et al., *Nat. Photonics.* **2007**, *1*, 336.
[14] E. Allaria, C. Callegari, D. Cocco, W. M. Fawley, M. Kiskinova, C. Masciovecchio, F. Parmigiani, *New J. Phys.* **2010**, *12*, 075002.
[15] W. Decking, S. Abeghyan, P. Abramian, A. Abramsky, A. Aguirre, C. Albrecht, P. Alou, M. Altarelli, P. Altmann, K. Amyan, V. Anashin, E. Apostolov, K. Appel, D. Auguste, V. Ayvazyan, S. Baark, F. Babies, N. Baboi, P. Bak, V. Balandin, R. Baldinger, B. Baranasic, S. Barbanotti,

 

O. Belikov, V. Belokurov, L. Belova, V. Belyakov, S. Berry, M. Bertucci, B. Beutner, et al., *Nat. Photonics.* **2020**, *14*, 650.
[16] P. Emma, R. Akre, J. Arthur, R. Bionta, C. Bostedt, J. Bozek, A. Brachmann, P. Bucksbaum, R. Coffee, F.-J. Decker, Y. Ding, D. Dowell, S. Edstrom, A. Fisher, J. Frisch, S. Gilevich, J. Hastings, G. Hays, Ph. Hering, Z. Huang, R. Iverson, H. Loos, M. Messerschmidt, A. Miahnahri, S. Moeller, H.-D. Nuhn, G. Pile, D. Ratner, J. Rzepiela, D. Schultz, et al., *Nat. Photonics.* **2010**, *4*, 641.
[17] T. Ishikawa, H. Aoyagi, T. Asaka, Y. Asano, N. Azumi, T. Bizen, H. Ego, K. Fukami, T. Fukui, Y. Furukawa, S. Goto, H. Hanaki, T. Hara, T. Hasegawa, T. Hatsui, A. Higashiya, T. Hirono, N. Hosoda, M. Ishii, T. Inagaki, Y. Inubushi, T. Itoga, Y. Joti, M. Kago, T. Kameshima, H. Kimura, Y. Kirihara, A. Kiyomichi, T. Kobayashi, C. Kondo, et al., *Nat. Photonics.* **2012**, *6*, 540.
[18] H.-S. Kang, C-Ki Min, H. Heo, C. Kim, H. Yang, G. Kim, I. Nam, S. Y. Baek, H.-J. Choi, G. Mun, B. R. Park, Y. J. Suh, D. C. Shin, J. Hu, J. Hong, S. Jung, S.-H. Kim, K. Kim, D. Na, S. S. Park, Y. J. Park, J.-H. Han, Y. G. Jung, S. H. Jeong, H. G. Lee, S. Lee, S. Lee, W.-W. Lee, B. Oh, H. S. Suh, et al., *Nat. Photonics.* **2017**, *11*, 708.
[19] E. Prat, R. Abela, M. Aiba, A. Alarcon, J. Alex, Y. Arbelo, C. Arrell, V. Arsov, C. Bacellar, C. Beard, P. Beaud, S. Bettoni, R. Biffiger, M. Bopp, H.-H. Braun, M. Calvi, A. Cassar, T. Celcer, M. Chergui, P. Chevtsov, C. Cirelli, A. Citterio, P. Craievich, M. C. Divall, A. Dax, M. Dehler, Y. Deng, A. Dietrich, P. Dijkstal, R. Dinapoli, et al., *Nat. Photonics.* **2020**, *14*, 748.
[20] J. S. Wojciech Gawelda, C. J. Milne, *X-Ray Spectroscopy at Free Electron Lasers*, John Wiley & Sons Ltd., Hoboken, NJ **2016**.
[21] M. Cammarata, R. Bertoni, M. Lorenc, H. Cailleau, S. Di Matteo, C. Mauriac, S. F. Matar, H. Lemke, M. Chollet, S. Ravy, C. Laulhé, J.-F. Létard, E. Collet, *Phys. Rev. Lett.* **2014**, *113*, 227402.
[22] H. T. Lemke, C. Bressler, L. X. Chen, D. M. Fritz, K. J. Gaffney, A. Galler, W. Gawelda, K. Haldrup, R. W. Hartsock, H. Ihee, J. Kim, K. H. Kim, J. H. Lee, M. M. Nielsen, A. B. Stickrath, W. Zhang, D. Zhu, M. Cammarata, *J. Phys. Chem. A.* **2013**, *117*, 735.
[23] H. T. Lemke, K. S. Kjær, R. Hartsock, T. B. van Driel, M. Chollet, J. M. Glownia, S. Song, D. Zhu, E. Pace, S. F. Matar, M. M. Nielsen, M. Benfatto, K. J. Gaffney, E. Collet, M. Cammarata, *Nat. Commun.* **2017**, *8*, 15342.
[24] Y. Obara, H. Ito, T. Ito, N. Kurahashi, S. Thurmer, H. Tanaka, T. Katayama, T. Togashi, S. Owada, Y. Yamamoto, S. Krashima, J. Nishitani, M. Yabashi, T. Suzuki, K. Misawa, *Struct Dynam.* **2017**, *4*, 044033.
[25] T. J. Penfold, J. Szlachetko, W. Gawelda, F. G. Santomauro, A. Britz, T. B. van Driel, L. Sala, S. Ebner, S. H. Southworth, G. Doumy, A. M. March, C. S. Lehmann, T. Katayama, M. Mucke, D. Iablonskyi, Y. Kumagai, G. Knopp, K. Motomura, T. Togashi, S. Owada, M. Yabashi, J. Rittmann, M. M. Nielsen, M. Pajek, K. Ueda, M. Chergui, R. Abela, C. J. Milne, in *Int.Conf. on Ultrafast Phenomena* Optica Publishing Group, Santa Fe, New Mexico **2016**, p. UF1A6.
[26] Y. Uemura, D. Kido, Y. Wakisaka, H. Uehara, T. Ohba, Y. Niwa, S. Nozawa, T. Sato, K. Ichiyanagi, R. Fukaya, S.-I. Adachi, T. Katayama, T. Togashi, S. Owada, K. Ogawa, M. Yabashi, K. Hatada, S. Takakusagi, T. Yokoyama, B. Ohtani, K. Asakura, *Angew. Chem., Int. Ed.* **2016**, *55*, 1364.
[27] J. Chen, H. Zhang, I. V. Tomov, M. Wolfsberg, X. Ding, P. M. Rentzepis, *J. Phys. Chem. A.* **2007**, *111*, 9326.
[28] M. Levantino, H. T. Lemke, G. Schiro, M. Glownia, A. Cupane, M. Cammarata, *Struct Dynam.* **2015**, *2*, 041713.
[29] N. A. Miller, A. Deb, R. Alonso-Mori, B. D. Garabato, J. M. Glownia, L. M. Kiefer, J. Koralek, M. Sikorski, K. G. Spears, T. E. Wiley, D. Zhu, P. M. Kozlowski, K. J. Kubarych, J. E. Penner-Hahn, R. J. Sension, *J. Am. Chem. Soc.* **2017**, *139*, 1894.
[30] N. A. Miller, A. Deb, R. Alonso-Mori, J. M. Glownia, L. M. Kiefer, A. Konar, L. B. Michocki, M. Sikorski, D. L. Sofferman, S. Song, M. J. Toda, T. E. Wiley, D. Zhu, P. M. Kozlowski, K. J. Kubarych, J. E. Penner-Hahn, R. J. Sension, *J. Phys. Chem. A.* **2018**, *122*, 4963.
[31] Y. Obara, T. Katayama, Y. Ogi, T. Suzuki, N. Kurahashi, S. Karashima, Y. Chiba, Y. Isokawa, T. Togashi, Y. Inubushi, M. Yabashi, T. Suzuki, K. Misawa, *Opt. Express.* **2014**, *22*, 1105.
[32] D. Zhu, M. Cammarata, J. M. Feldkamp, D. M. Fritz, J. B. Hastings, S. Lee, H. T. Lemke, A. Robert, J. L. Turner, Y. Feng, *Appl. Phys. Lett.* **2012**, *101*, 034103.
[33] M. Harmand, A. Ravasio, S. Mazevet, J. Bouchet, A. Denoeud, F. Dorchies, Y. Feng, C. Fourment, E. Galtier, J. Gaudin, F. Guyot, R. Kodama, M. Koenig, H. J. Lee, K. Miyanishi, G. Morard, R. Musella, B. Nagler, M. Nakatsutsumi, N. Ozaki, V. Recoules, S. Toleikis, T. Vinci, U. Zastrau, D. Zhu, A. Benuzzi-Mounaix, *Phys. Rev. B.* **2015**, *92*, 024108.
[34] M. Harmand, M. Cammarata, M. Chollet, A. G. Krygier, H. T. Lemke, D. L. Zhu, *Sci. Rep.* **2023**, *13*, 18203.
[35] Y. Ogi, Y. Obara, T. Katayama, Y.-I. Suzuki, S. Y. Liu, N. C.-M. Bartlett, N. Kurahashi, S. Karashima, T. Togashi, Y. Inubushi, K. Ogawa, S. Owada, M. Rubesová, M. Yabashi, K. Misawa, P. Slavicek, T. Suzuki, *Struct. Dyn.* **2015**, *2*, 034901.
[36] S. Reiche, C. Bacellar, P. Bougiatioti, C. Cirelli, P. Dijkstal, E. Ferrari, P. Juranic, G. Knopp, A. Malyzhenkov, C. Milne, K. Nass, E. Prat, J. Vila-Comamala, C. David, *Phys. Rev. Res.* **2023**, *5*, L022009.
[37] E. Prat, P. Dijkstal, M. Aiba, S. Bettoni, P. Craievich, E. Ferrari, R. Ischebeck, F. Löhl, A. Malyzhenkov, G. L. Orlandi, S. Reiche, T. Schietinger, *Phys. Rev. Lett.* **2019**, *123*, 234801.
[38] C. Milne, T. Schietinger, M. Aiba, A. Alarcon, J. Alex, A. Anghel, V. Arsov, C. Beard, P. Beaud, S. Bettoni, M. Bopp, H. Brands, M. Brönnimann, I. Brunnenkant, M. Calvi, A. Citterio, P. Craievich, M. Csatari Divall, M. Dällenbach, M. D'Amico, A. Dax, Y. Deng, A. Dietrich, R. Dinapoli, E. Divall, S. Dordevic, S. Ebner, C. Erny, H. Fitze, U. Flechsig, et al., *Appl. Sci.* **2017**, *7*, 720.
[39] Y. Obara, T. Katayama, Y. Ogi, T. Suzuki, N. Kurahashi, S. Karashima, Y. Chiba, Y. Isokawa, T. Togashi, Y. Inubushi, M. Yabashi, T. Suzuki, K. Misawa, in *19th Int. Conf. on Ultrafast Phenomena*, Optica Publishing Group, Okinawa **2014**, p. 07MonB7.
[40] C. David, B. Nohammer, E. Ziegler, *Appl. Phys. Lett.* **2001**, *79*, 1088.
[41] M. Makita, P. Karvinen, V. A. Guzenko, N. Kujala, P. Vagovic, C. David, *Microelectron. Eng.* **2017**, *176*, 75.
[42] P. Juranic, J. Rehanek, C. A. Arrell, C. Pradervand, A. Cassar, M. Calvi, R. Ischebeck, C. Erny, P. Heimgartner, I. Gorgisyan, V. Thominet, K. Tiedtke, A. Sorokin, R. Follath, M. Makita, G. Seniutinas, C. David, C. J. Milne, H. Lemke, M. Radovic, C. P. Hauri, L. Patthey, *J. Synchrotron Radiat.* **2019**, *26*, 906.
[43] https://docs.xrayabsorption.org/xaslib/ (accessed: July 2023).
[44] H. Yoneda, Y. Inubushi, M. Yabashi, T. Katayama, T. Ishikawa, H. Ohashi, H. Yumoto, K. Yamauchi, H. Mimura, H. Kitamura, *Nat. Commun.* **2014**, *5*, 5080.

 